Metallurgy and materials
Metalurgia e materiais

Effect of cold-working process on cyclic deformation of electrolytic copper

http://dx.doi.org/10.1590/0370-44672018720157

Gustavo Aristides Santana Martinez[1,3]
https://orcid.org/0000-0002-7870-9269
Carlos Antônio Reis Pereira Baptista[2,4]
https://orcid.org/0000-0001-5762-8235

[1]Universidade de São Paulo - USP, Escola de Engenharia de Lorena - EEL , Departamento de Ciências Básicas e Ambientais - DEBAS, Lorena - São Paulo - Brasil.

[2]Universidade de São Paulo - USP, Escola de Engenharia de Lorena - EEL, Departamento de Engenharia de Materiais - DEMAR, Lorena - São Paulo - Brasil.

E-mails: [3]gustavo.martinez@usp.br, [4]carlos.baptista@usp.br

Abstract

Cyclic softening and hardening processes are expressed by the change in the stress amplitude necessary to cause a given strain amplitude. Understanding the cyclic stress-strain behavior of materials is an important step in the complex study of their fatigue behavior. The potential differences between the defect structures of cold-formed materials may also be related to internal stress changes. Considering that wiredrawing and rotary swaging apply distinct forces on the material in order to obtain the product, differences may arise in the defect structures that can, consequently, affect its mechanical behavior. This study aims at evaluating and comparing, by means of strain-controlled fatigue tests, the cyclic behavior of polycrystalline electrolytic copper cold-formed by wiredrawing (WD) and rotary swaging (RS) with 87% area reduction. The fatigue test results evidenced the highest resistance to cyclic deformation presented by WD material in the low cycle regime. It was observed that the strain hardening for both cold forming conditions is related to a great increase of long-range stresses in the defect structure and the cyclic softening is related, mainly, to the subsequent drop of that stresses. The WD internal stresses resulted slightly bigger than those of the RS condition.

Keywords: drawing, rotary swaging, fatigue, cyclic behavior, copper.

1. Introduction

Understanding the cyclic stress-strain behavior of materials is an important step in the complex study of their fatigue behavior. The cyclic deformation of copper has been the subject of many researches; notwithstanding, most of the investigations are focused on annealed copper and in nanocrystalline material (Jain, 1990; Guo *et al*., 2005; Maier and Gabor, 2005; Seifi and Hosseini, 2018; Chen *et al*., 2018). The study of cyclic plasticity includes investigations on the dislocation structures and the stress-strain relationships. The most significant changes triggered by the cyclic deformation refer to the mechanical properties of the material and can be evaluated through continuous measures of the hysteresis loop during the cyclic loading in strain-controlled testing. Depending on the component's initial state, the material might suffer cyclic hardening or softening, or even keep a steady state regime. It is not uncommon to observe distinct behavior characteristics in the same material, depending on the initial conditions and the cyclic loading parameters (Carstensen, 1998; Howard *et al*., 2017). Fatigue softening is the reduction of tensile strength in cold worked metals caused by cyclic loading and understood in terms of the internal structure of the metal.

Among the techniques available for the fatigue life prediction of materials and components, the strain-life approach (ε/N) stands out, since it considers the high cycle (described by Basquin's law) and low cycle fatigue (Coffin-Manson's equation) in a unique expression, besides being used in local strain analysis. Hence, strain acting at the critical point of the components is considered, due to stress concentration, to foresee the number of cycles to failure (Conway and Sjodahl, 1991; Klesnil and Lukas, 1992). In this approach, the total deformation amplitude ε_{at} observed in the hysteresis loop is considered in relation to its elastic ε_{ae} and plastic ε_{ap} portions, expressed by equation (1). The cyclic softening and hardening of the material can be evaluated by the cyclic stress-strain curve (CSSC). The cyclic stress-strain behavior of raw and annealed pure copper has been also taken in account in fatigue crack growth studies (Seifi and Hosseini, 2018). The tips from a family of multiple hysteresis loops measured at distinct strain amplitudes can be connected to form the CSSC, which is described by equation (2), where E is the Young's modulus, K' is the cyclic strength coefficient and n' is the cyclic hardening exponent (Dowling *et al*., 2018). The widely accepted representation of the fatigue curve was proposed by Morrow (1965) and is given by equation (3), where E is the Young's modulus, $2N_f$ is the number of reversions to failure, σ'_f and ε'_f are the fatigue strength and ductility coefficients and b, c are respectively the fatigue strength and ductility exponents.

$$\varepsilon_{at} = \varepsilon_{ae} + \varepsilon_{ap} \quad (1)$$

$$\varepsilon_{at} = \frac{\sigma_a}{E} + \left(\frac{\sigma_a}{K'}\right)^{1/n'} \quad (2)$$

$$\varepsilon_{at} = \frac{\sigma'_f}{E}(2N_f)^b + \varepsilon'_f(2N_f)^c \quad (3)$$

Cyclic softening and hardening processes are expressed by the change in the stress amplitude necessary to cause a given strain amplitude. Even for the fatigue life portions in which the peak stress remains constant, a continuous microstructural change occurs in the material. The applied external stress must be in equilibrium with the internal stresses, which can be subdivided according to the distance in which they are effective. Two internal stress parameters, obtained directly from the hysteresis loop, are often used in the study of the cyclic behavior of metallic materials. The concept of internal stresses appears both in viscoplastic models of continuum mechanics as well as in microscopic theories of deformation (Jain, 1990).

In the microscopic approach, the two variables usually chosen are the friction stress and the back stress. The friction stress σ_f is the stress required locally for a dislocation to move and is mainly related with short-range obstacles such as the lattice friction. The back stress σ_b provides a long-range interaction with mobile dislocations and is mainly related to the microstructural barriers or strain incompatibilities in the material (Xu *et al.,* 2017). In Metallurgical terminology, this refers to the stress that arises against the dislocation movement due to the stacking of same signal dislocations. While σ_f is independent of the strain, σ_b changes its signal on each reversion. It always attains the maximum value at the point of maximum cyclic strain, acting to reduce the flow stress in reverse. Being of elastic nature, the back stress decreases during the reversed deformation and then increases again in the opposite direction, in order to resist the continuity of deformation (Kuhlmann-Wilsdorf and Laird, 1979; Feaugas and Clavel, 1997). Therefore, internal stresses are defined on the basis of dislocation behavior during plastic deformation and are empirically related to the microstructural quantities, such as grain size and dislocation density. Recently it was shown, for example, that the grain size has a significant effect on the development of back stress in polycrystalline copper (Mahato *et al.,* 2016). The internal stresses evolve during plastic deformation as various mobile dislocations, and immobile dislocation configurations, such as tangles, forests and cells interact with one and another by the processes of multiplication, annihilation, immobilization and remobilization. A relatively simple technique for the measurement of friction and back stresses is referred to in literature as the KWL method, which was proposed by Kuhlman-Wilsdorf and Laird (1979). Considering the peak stress as the stress amplitude in the loading cycle, σ_a, and denoting the flow stress by σ_e, the friction and back stresses can be estimated with equations (4) and (5) (Meininger and Gibeling, 1992).

$$\sigma_f = \frac{(\sigma_a - \sigma_e)}{2} \quad (4)$$

$$\sigma_b = \frac{(\sigma_a + \sigma_e)}{2} \quad (5)$$

Polycrystalline copper has been studied frequently in both high and low cycle fatigue, as well as for its fatigue crack growth resistance (Guo *et al.,* 2005; Marnier *et al.,* 2016; Seifi and Hosseini, 2018). The evolution of internal stresses in samples of polycrystalline annealed copper has been analyzed by using the KWL technique (Dickson *et al.,* 1984; Jain, 1990; Carstensen, 1998). Studies were performed by applying distinct deformation rates and plastic strain amplitudes. Various parameters, as the asymmetry of the cyclic yield stress and the internal stress evolution were observed. Results were discussed in terms of dislocation dynamics.

The cold deformation process may affect the physical and mechanical properties of copper. It was shown, for instance, that the machine speed caused great impact on electrical properties of copper deformed by cold drawing (Bernardo and Fernandes Neto, 2017). The potential differences between the defect structures of cold-formed materials may also be related to internal stress changes (Mughrabi *et al.,* 1981). This fact encourages the investigation about the cyclic behavior of cold-worked copper, relating the low cycle fatigue properties and internal stresses to the processing route.

Considering that wiredrawing and rotary swaging apply distinct forces on the material in order to obtain the product, differences may arise in the defect structures that can, consequently, affect its mechanical behavior. This work aims at evaluating and comparing, by means of strain-controlled fatigue tests, the cyclic behavior of polycrystalline electrolytic copper cold-formed by wiredrawing and rotary swaging with 87% area reduction.

2. Material and method

The initial material condition for this study was an annealed bar of electrolytic copper (99.94% Cu in weight), with diameter 25.4 mm, non-pickled and totally free of any surface treatment. Two segments of the bar with 1000 mm length were cold-formed to the final diameter of 9.0 mm (87% area reduction), each of them by a single process: wiredraw-

ing and rotary swaging. The obtained material conditions are referred to herein as RS (cold-rotary swaged material) and WD (cold wiredrawn material). In both processes, the forming speed was 0.1 m/s. Wiredrawing was performed in a Schumag machine of simple pass and controlled speed using hard metal dies. Rotary swaging was performed in a FENN machine, model 3F, of four dies, power of about 30 Cv and speed of 1700 revolutions per minute. In a previous study, the microstructure, microhardness, texture and corrosion resistance of the copper rods obtained by both RS and WD, were determined and compared to each other (Robin *et al.*, 2012). Both forming processes resulted in microstructures in which the copper grains were elongated along the cold-working direction, see Figure 1. Although the microstructures of WD and RS conditions are very similar, the deformation seems to have been more homogeneous for the wiredrawn rods. Besides, the corrosion resistance of WD rods investigated in H_2SO_4 solutions was lower than that of the RS ones.

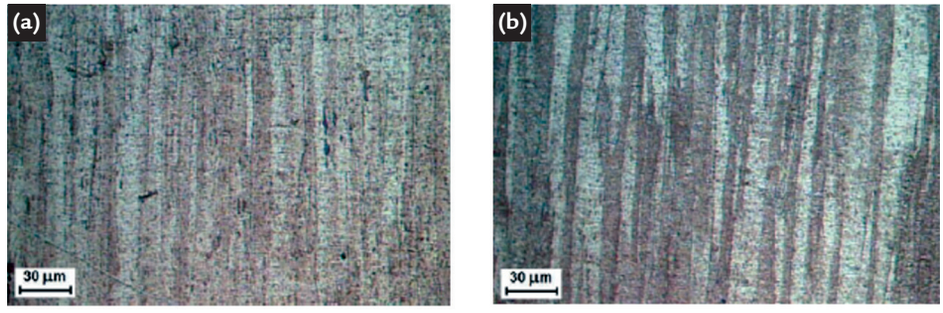

WD RS

Figure 1
Microstructures of the 9 mm copper rods (Robin et al., 2012).

The Vickers micro hardness numbers for both material conditions are the following: for WD material, HV = 113.8 ± 3.5, and for the RS condition, HV = 102.1 ± 3.0. It is known that the area reduction results in moving and increasing the density of grain boundaries, which explains the micro hardness increase compared to the annealed copper (HV = 99.5 ± 3.4). The standard deviation of hardness indicates the homogeneity level for each process and the way that the plastic flow of the material occurs explains the differences between the hardness values (Robin *et al.,* 2012). In the WD condition, deformation occurs by the application of radial compressive stress associated with axial tractive stress, which generates a high concentration of stored energy and, consequently, high mechanical hardness.

In order to accomplish the static characterization of the material, the monotonic mechanical properties of the cold formed bars, i.e., Young's modulus (E), yield stress (σ_{ys}) and ultimate tensile strength (σ_u), were determined by means of tensile tests. Small-size round test-pieces with diameter of 6.0 mm and gage length of 30 mm were employed and the adopted testing speed was 0.5 mm/min. The results (mean values from three tests for each material condition) are shown in Table 1. The higher strength of WD metals compared to the RS ones has also been observed elsewhere (Brandão and Kalu, 1998).

Table 1
Mechanical properties of cold WD and RS copper.

Material Condition	E (GPa)	σ_{ys} (MPa)	σ_u (MPa)
WD	117	444	456
RS	119	376	397

Cylindrical fatigue specimens with gage section of 4.0 mm in diameter and 10.0 mm in length were machined and finished by using 400-800 grit silicon carbide emery paper. Low-cycle fatigue tests were performed at room temperature in laboratory air by using a MTS servo-hydraulic machine with total strain control mode, frequency of 0.5 Hz and totally reversed cycles with strain amplitudes within the range 0.2 to 2.0%. During the tests, data acquisition was performed in order to obtain about 200 experimental points on each elasto-plastic hysteresis loop collected. Elastic and plastic portions of deformation were determined from the hysteresis loops according to the method of AECMA (Kandil, 1999). Low cycle fatigue properties were calculated by using equations (2) and (3). Internal stresses were determined by following KWL method. It is important to note that the flow stress value is somehow arbitrary, since it depends on the method adopted to define the start of plastic deformation. This limitation does not prevent that, since the same criteria along the performed tests is adopted, especially if the relative values of friction and back stresses calculated by equations (4) and (5) are significant (Meininger and Gibeling, 1992). In this study, we used *offset* of 0.1% to obtain the flow stress values.

3. Results and discussion

The cyclic stress response during strain controlled cyclic loading is shown in Figure 2 for the WD (a) and RS (b) material conditions. After a very short (less than 10 reversals) hardening, both conditions suffer a continuous and pronounced softening. It is known that the fatigue softening caused by axial tension and compression occurs mainly in FCC metals, like copper, whose stacking fault energy is high enough to allow cross-slip. In the softening process, the dislocations rearrange by cross-slipping during cyclic loading and form a subgrain structure so plastic flow can occur at lower stresses within the microstructure than in the prior work hardened condition. On Figure 2, we can also notice that for the WD condition, six of the nine tested specimens achieved peak stresses above 400 MPa, whereas for

the RS condition, the maximum peak stresses were equal to or lower than 400 MPa for six of the nine specimens. This result is in accordance to the higher strength shown by the WD condition in the tensile test, see Table 1.

Cyclic properties of the material were determined from half-life hysteresis loops and are shown in Table 2. Parameters of the CSSC defined by equation (2) were determined by numerical fitting of the corresponding points regarding the peaks of the hysteresis loops. values can be compared to the results of the annealed copper (99.9% purity), presented by K' = 396 MPa and n' = 0.10 (Plumtreee and Abdel-Raouf, 2001). The annealed material presents a lower strength coefficient although the cyclic hardness exponent is close to the RS material. The lower value of n' for the WD condition can be associated to a more stable cyclic deformation behavior.

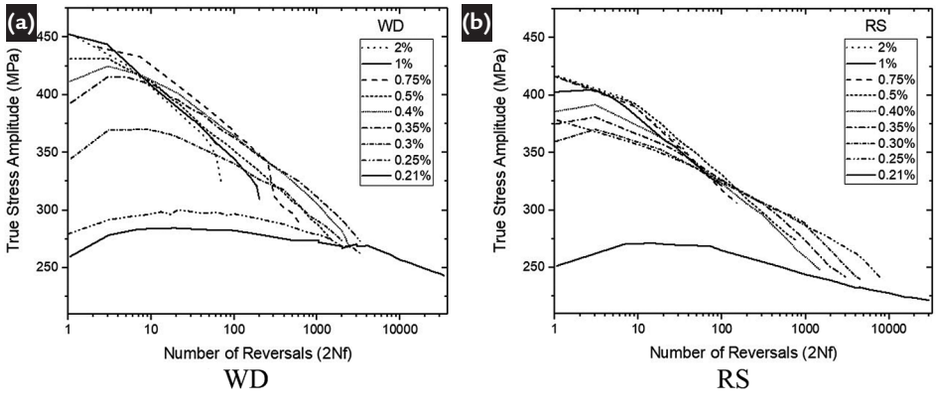

Figure 2
Cyclic softening curves for material conditions.

Condition	K'	n'	σ'_f	*b*	ε'_f	*c*
WD	485.8	0.0781	299.5	-0.0296	0.382	-0.677
RS	552.9	0.1140	350.0	-0.0580	0.129	-0.522

Table 2
Cyclical properties of the material conditions.

The low cycle fatigue curves for WD and RS conditions are shown in Figure 3. It is observed that the transition life (intersection between the elastic and plastic lines) is approximately 2×10^3 reversals for WD and 3×10^3 for RS conditions. This transition occurs, in both cases, at a total strain amplitude a little above 2×10^{-3}. The lower plastic strain amplitude associated to a certain total cyclic deformation level is determinant so that the WD material presents, in the low cycle section, a fatigue life higher than the RS material as shown in Figure 4.

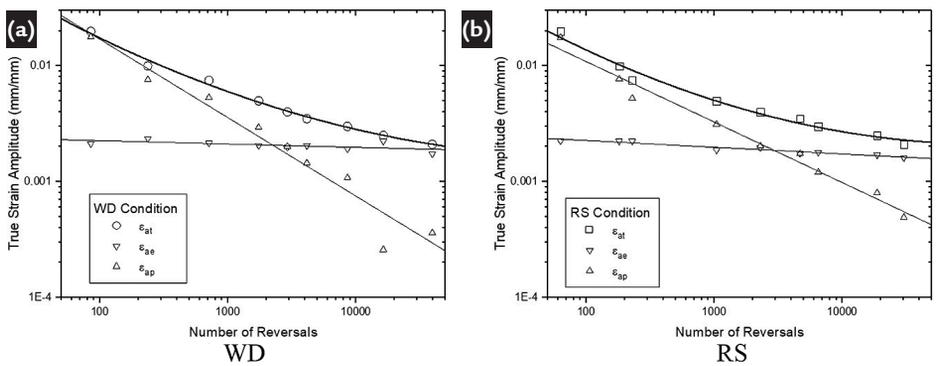

Figure 3
Low cycle fatigue curves for electrolytic copper.

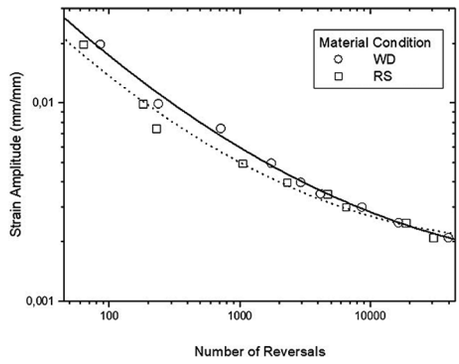

Figure 4
Comparison of strain-life curves for electrolytic copper in WD and RS conditions.

The half-life hysteresis loops collected from the tests were translated to a common point of maximum compressive stress, as shown in Figure 5. The plots in Figure 5 show that both material conditions deviate from the Masing behavior, in which the hysteresis loop branches fall on the same curve for all strain levels (Borrego *et al.*, 2004). Masing behavior is a characteristic of low stacking fault energy, and for some of such materials, the defect sub-

structure consists of a planar array of dislocations. High stacking fault energy materials, like copper, deviate from the Masing behavior and the plastic strain representing the onset of the non-Masing behavior increasing inversely with the stacking-fault energy. Plumtree and Abdel-Raouf (2001) found this threshold to be 0.005 for commercial purity copper and the plots shown in Figure 5 appear to agree with this value. Besides that, WD material shows higher peak stresses in half-life hysteresis loops in almost all of the tested strain amplitudes. On the other hand, the hysteresis loops for both material conditions tested at 2% strain amplitude virtually superpose each other, indicating that higher strain amplitudes can supplant the effects of the different plastic flow modes in the cyclic behavior of the material.

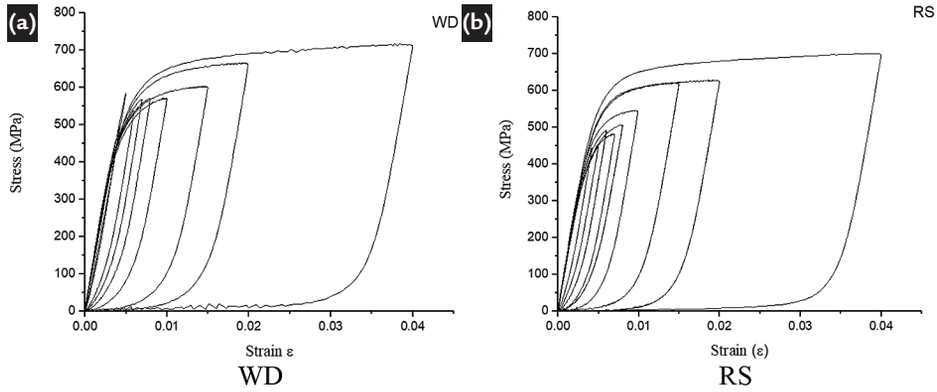

Figure 5
Superimposed stress-strain loops with matched lower tips.

Analyses of internal stresses according to the KWL method indicated that, for the tested cyclic strain amplitudes, the back stress was maintained systematically higher than the friction stress, which is a typical characteristic of strain-hardened materials. A detailed analysis was performed for tests with a total deformation amplitude of 0.5%. Figure 6 features that the evolution of hysteresis loops during the tests is similar for the two conditions of the material, in the characteristic of cyclic softening. Using these hysteresis loops and adopting an offset of 0.1%, friction and back stresses were determined and plotted against the number of reversions corresponding to each loop, as shown in Figure 7.

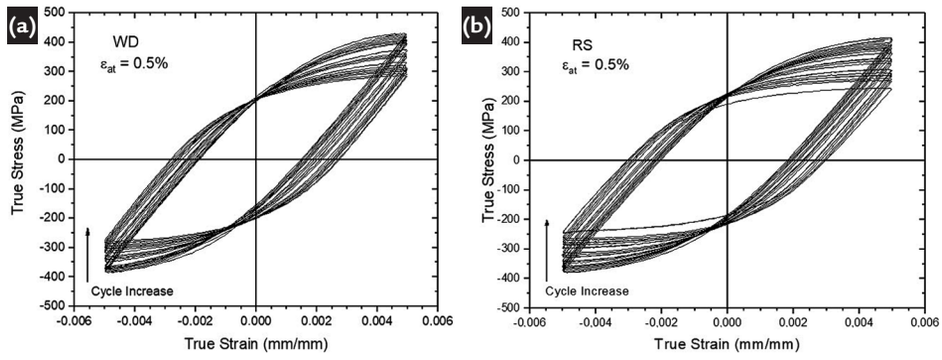

Figure 6
Stress-strain behavior of copper subjected to 0.5% cyclic strain amplitude.

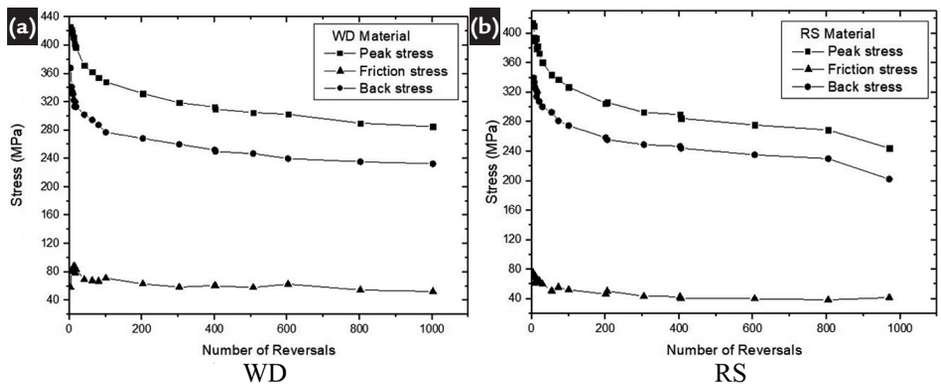

Figure 7
Internal stresses evolution with cyclic deformation for both material conditions.

Figure 7 features that the friction stress starts from values between 60 and 90 MPa at the onset of cycling and slightly decreases during the test, reaching values around 50 MPa for both conditions of the material. The values here determined for friction stress are of the same magnitude as the ones obtained by Dickson *et al.* (1984) for annealed polycrystalline copper cycled with deformation amplitude of 0.4%, approximately 80 MPa. On the other hand, the back stress values are between 330-350 MPa at the onset of cycling and drops to 240-250 MPa with accumulated plastic deformation. The back stress, which is related to the level of hardening, is significantly higher than that obtained for annealed copper (a material condition that cyclically hardens and has a tendency towards saturation), which is around 70 MPa (Dickson *et al.*, 1984).

According to results obtained in this study, the strain hardening due to cold forming of copper is related to a great increase of long-range stresses in the defect structure and the cyclic softening is related, mainly, to the subsequent drop of these stresses. Values of internal stresses of the WD material are slightly bigger than those of the RS condition.

The two material conditions featured significant differences in the cracking process. Figure 8 shows fractographies obtained via scanning electron microscopy of WD and RS samples tested at 0.5% total strain amplitude. We should note that, after nucleation and initial growth of the fatigue crack, the peak stress drops sharply, stopping the test for failure. Therefore, the remaining section was split into two parts by tensile loading to fracture after the test was finished. Pictures shown in Figure 8, for both tests, feature the nucleation of one main crack that grew to about 1/3 of the specimen test section. The detail pictures zoomed at 200 X show the transition between the fatigue crack growth and the final fracture region. It can be observed that, for WD condition, fatigue striation is less noticeable and presents lower spacing than for RS condition. Besides that, the final fracture of WD sample features a prominent dimpled characteristic, indicating a higher deformation ability. These characteristics are in accordance with greater resistance to cyclic deformation presented by WD condition in regard to the RS condition.

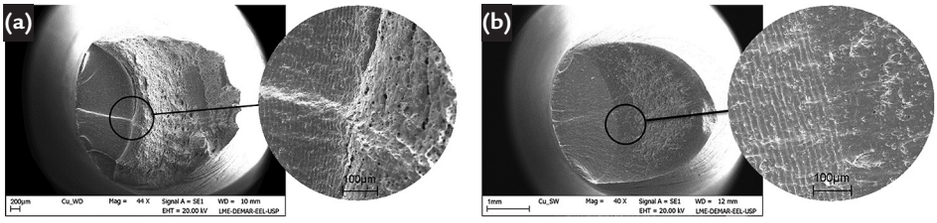

WD RS

Figure 8
SEM fractography of WD and RS copper rods tested at 0.5% strain amplitude.

4. Conclusions

In this study, the cyclic stress-strain behavior of copper rods processed by cold wiredrawing (WD) and rotary swaging (RS) were compared. The cyclic response of both WD and RS conditions is characterized by a continuous and pronounced softening from peak stresses around 400 MPa and within a wider range for the WD condition. The CSSC parameters show higher strength coefficients of both cold-formed conditions in comparison to the annealed material. The WD condition presented a cyclic hardening exponent of 0.078, lower than the value 0.114 found for the RS material, due to the higher stresses at saturation presented by the former at strain amplitudes of 0.5% and below. The fatigue properties produced the highest resistance to cyclic deformation presented by WD material in the low cycle regime, regardless of its lower corrosion resistance shown in a previous article. It was observed that the strain hardening for both cold forming conditions is related to a great increase of long-range stresses in the defect structure and the cyclic softening is related, mainly, to the subsequent drop of these stresses. Moreover, the WD internal stresses resulted slightly bigger than those of the RS condition. In accordance to its higher fatigue resistance, the WD fracture surfaces presented a less noticeable and lower spacing striation than the RS condition.

References

BERNARDO, R. S., FERNANDES NETO, M. Influence of a cold deformation process by drawing on the electrical properties of copper wires. ***REM - International Engineering Journal,*** v. 70, p. 53-57, 2017.

BORREGO, L. P., ABREU, L. M., COSTA, J. M., FERREIRA, J. M. Analysis of low cycle fatigue in AlMgSi aluminum alloys. ***Engineering Failure Analysis,*** v. 11, p. 715-725, 2004.

BRANDÃO, L., KALU, P.N. The effect of fabrication mode on microstructure, texture and strength in Cu–Nb/Ti composite. ***Scripta Mater,*** v. 39, p. 27–33, 1998.

CARSTENSEN, J. V. ***Structural evolution and mechanisms of fatigue in polycrystalline brass.*** Roskilde, Denmark: Riso National Laboratory, 1998. 145p. (DCAMM report-Doctoral Thesis).

CHEN, W., KITAMURA, T., WANG, X., FENG, M. Size effect on cyclic torsion of micropolycrystalline copper considering geometrically necessary dislocation and strain gradient. ***International Journal of Fatigue,*** v. 117, p. 292-298, 2018.

CONWAY, J. B., SJODAHL, L. H. Analysis and representation of fatigue data. ***Materials Park,*** Ohio: ASM International, 1991.

DICKSON, J. I., BOUTIN, J., HANDFIELD, L. A comparison of two simple methods for measuring cyclic internal and effective stresses. ***Materials Science and Engineering,*** v. 64, p. L7-L11, 1984.

DOWLING, N. E., KAMPE, S. L., KRAL, M. V. ***Mechanical behavior of***

materials. (5 ed.). Hoboken: Pearson Education, 2018.

FEAUGAS, X., CLAVEL, M. Cyclic deformation behavior of an α/β titanium alloy I: micromechanisms of plasticity under various loadings paths. ***Acta Materialia,*** v. 45, n. 7, p.2685-2701, 1997.

GUO, X. L., LU, L., LI, S. X. Cyclic deformation behavior in pure Cu with growth-in twins. ***Materials Science and Engineering A,*** v. 405, p. 239-245, 2005.

HOWARD, C., FRITZ, R., ALFREIDER, M., KIENER, D., HOSEMANN, P. The influence of microstructure on the cyclic deformation and damage of copper and an oxide dispersion strengthened steel studied via in-sito micro-beam bending. ***Materials Science and Engineering: A,*** v. 687, p.313-322, 2017.

JAIN, M. Evolution of internal stress variables during cyclic deformation of copper. ***Materials Science and Engineering: A,*** v. 128, n. 2, p. 183-193, 1990.

KANDIL, F. A. Potential ambiguity in the determination of the plastic strain range component in LCF testing. ***International Journal of Fatigue,*** v. 21, p. 1013-1018, 1999.

KLESNIL, M., LUKÁŠ, P. ***Fatigue of metallic materials.*** (2 ed.). Amsterdam: Elsevier, 1992.

KUHLMANN-WILSDORF, D., LAIRD, C. Dislocation behavior in fatigue II: friction stress and back stress as inferred from an analysis of hysteresis loops. ***Materials Science and Engineering,*** v. 37, p. 111-120, 1979.

MAHATO, J. K., SARATHI, P., SARKAR, A., KUNDU, A., CHAKRABORTI, P. C. Effect of deformation mode and grain size on Bauschinger behavior of annealed copper. ***International Journal of Fatigue,*** v. 83, p. 42-52, 2016.

MAIER, H. J., GABOR, P. Cyclic stress-strain response and low-cycle fatigue damage in ultrafine grained copper. ***Materials Science and Engineering A,*** v. 410-11, p. 457-461, 2005.

MARNIER, G., KELLER, C., TALEB, L. Fatigue of OFHC pure copper and 316L stainless steel subjected to prior tensile and cyclic prestrains. ***International Journal of Fatigue,*** v. 91, p. 204-219, 2016.

MEININGER, J. M., GIBELING, J. C. Low-cycle fatigue of niobium and niobium- 1Pct zirconium alloys. ***Metallurgical Transactions A,*** v. 23A, p. 3077-3084, 1992.

MORROW, J. Cyclic plastic strain energy and fatigue of metals. In: SYMPOSIUM OF INTERNAL FRICTION, DAMPING AND CYCLIC PLASTICITY, 1965, Chicago. Internal friction, damping, and cyclic plasticity. ***Philadelphia: American Society for Testing and Materials,*** 1965. p. 45-87. (ASTM STP 378).

MUGHRABI, H., HERZ, K., STARK, X. Cyclic deformation and fatigue behavior of alfa-Iron monoand polycrystals. ***International Journal of Fracture,*** v. 17, p. 193-220, 1981.

PLUMTREE, A., ABDEL-RAOUF, H. A. Cyclic stress-strain response and substructure. ***International Journal of Fatigue,*** v. 23, p. 799-05, 2001.

ROBIN, A., MARTINEZ, G. A. S., SUZUKI, P. A. Effect of cold-working process on corrosion behavior of cooper. ***Materials and Design,*** v. 34, p. 319-324, 2012.

SEIFI, R., HOSSEINI, R. Experimental study of fatigue crack growth in raw and annealed pure copper with considering cyclic plastic effects. ***Theoretical and Applied Fracture Mechanics,*** v. 94, n. 1-9, 2018.

XU, H., YE, D., MEI, L. A study of the back stress and the friction stress behaviors of Ti-6Al-4V alloy during low cycle fatigue at room temperature. ***Materials Science and Engineering A,*** v. 700, p. 530-539, 2017.

Received: 28 November 2018 - Accepted: 23 April 2019.